Branching ratios of $B^+ \to D^{(*)+} K^{(*)0}$ decays in the perturbative QCD approach

Ge-Liang Song* and Cai-Dian Lü†

CCAST (World Laboratory), P.O. Box 8730, Beijing 100080, China

and Institute of High Energy Physics, CAS, P.O. Box 918(4), Beijing 100039, China

(Received 22 March 2004; published 17 August 2004)

We study the rare decays $B^+ \to D^{(*)+} K^{(*)0}$, which can occur only via annihilation-type diagrams in the standard model. We calculate all of the four modes $B \to PP$, VP, PV, VV in the framework of the perturbative QCD approach and give the branching ratios of the order about 10^{-6}.

DOI: 10.1103/PhysRevD.70.034006 PACS number(s): 13.25.Hw, 11.10.Hi, 12.38.Bx

I. INTRODUCTION

More and more data of B decays are being collected at the two B factories Belle and BaBar. The original approach to nonleptonic B decays based on the factorization approach (FA) [1], which succeeded in calculating the branching ratios of many decays [2]. The FA is a simple method by which nonfactorizable and annihilation contributions are neglected. Although calculations are easy in the FA, it suffers the problems of scale, infrared-cutoff, and gauge dependence [3]. Especially it is difficult to explain some observed branching ratios of B decays, such as $B \to J/\psi K^{(*)}$ [4]. To improve the theoretical application [5] and understand why the simple FA works so well [6,7], some methods have been brought forward and developed. One of them is the perturbative QCD (PQCD) approach developed by Brodsky and Lepage [8,9], under which we can calculate the annihilation diagrams as well as the factorizable and nonfactorizable diagrams.

It is consistent to calculate branching ratios of B decays in the PQCD approach, as we will explain its framework in the next section. It has been applied in the nonleptonic B decays [6,7,10,11] successfully. In the case of $B^+ \to D^{(*)+} K^{(*)0}$ decays, which is a kind of pure annihilation-type decays, the physics picture of PQCD is as follows, shown in Fig. 1. A W boson exchange causes $\overline{b}u \to \overline{s}c$, and the $\overline{d}d$ quarks are produced from a gluon. In the rest frame of the B meson, the d and $\overline{d}$ quarks in the $D^{(*)+} K^{(*)0}$ mesons each has momentum $\mathcal{O}(M_B/4)$, so the gluon producing them has $q^2 \sim \mathcal{O}(M_B^2/4)$. It is a hard gluon according to the mass of the B meson. So we can perturbatively treat these decays and use the PQCD approach like other pure annihilation-type B decays [12].

In the next section, we explain the framework of PQCD briefly. In Sec. III, we give the analytic formulas for the decays $B^+ \to D^{(*)+} K^{(*)0}$. In Sec. IV, we show the numerical results and theoretical errors of the four modes, respectively. Finally, we draw a conclusion in Sec. V.

II. FRAMEWORK

The PQCD approach divides the process into hard components, which are treated by perturbative theory, and nonperturbative components, which are put into the hadron wave function. The hadron wave function can be extracted from experimental data or calculated by QCD sum rules method. The decay amplitude can be conceptually written as the convolution

$$\text{amplitude} \sim \int d^4k_1 d^4k_2 d^4k_3 \mathrm{Tr}[C(t)\Phi_B(k_1) \times \Phi_{D^{(*)}}(k_2)\Phi_{K^{(*)}}(k_3)H(k_1,k_2,k_3,t)], \quad (1)$$

where k_i's are momenta of light quarks included in each meson, and Tr denotes the trace over Dirac and color indices. The hard components comprise the hard part (H) and harder dynamics (C). $H(t)$ describes the four-quark operator and the spectator quark connected by a hard gluon. It can be perturbatively calculated, since it includes the hard dynamics characterized by the scale t, where $t \sim \mathcal{O}$ ($M_B/2$) for $B^+ \to D^{(*)+} K^{(*)0}$ decays, and the hard gluon's q^2 is of the or-

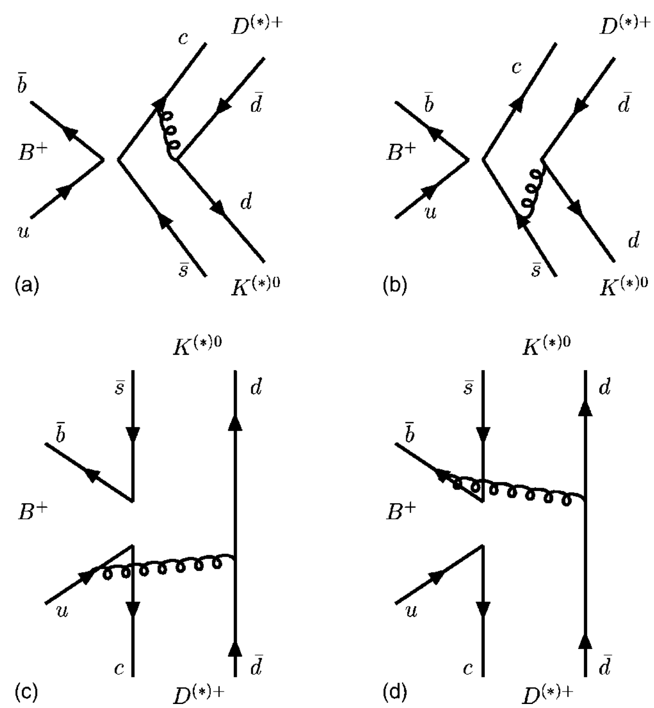

FIG. 1. Diagrams for $B^+ \to D^{(*)+} K^{(*)0}$ decays. The factorizable diagrams (a), (b) contribute to F, and nonfactorizable (c), (d) contribute to M.

*Email address: songgl@mail.ihep.ac.cn

†Email address: lucd@mail.ihep.ac.cn

der of t^2. $C(t)$ is the Wilson coefficient which results from the radiative corrections at short distance. In the above convolution, $C(t)$ includes the harder dynamics at a larger scale than the M_B scale and describes the evolution of local four-fermion operators from M_W down to the scale t. The wave function Φ_M denotes the nonperturbative components, which is independent of the specific processes and removes the infrared cutoff dependence in the PQCD approach.

For simplicity, we use the light-cone coordinate to describe the meson's momenta in the rest frame of the B meson. According to the conservation of four-momentum, we can obtain the B^+, $D^{(*)+}$, and $K^{(*)0}$ meson's momenta in the light-cone coordinate as

$$P_1=\frac{M_B}{\sqrt{2}}(1,1,\mathbf{0}_T),$$

$$P_2=\frac{M_B}{2\sqrt{2}}\left(\eta+\sqrt{\eta^2-4r_2^2},\quad \eta-\sqrt{\eta^2-4r_2^2},\ \mathbf{0}_T\right),$$

$$P_3=\frac{M_B}{2\sqrt{2}}\left(\xi-\sqrt{\xi^2-4r_3^2},\xi+\sqrt{\xi^2-4r_3^2},\ \mathbf{0}_T\right), \tag{2}$$

where $\eta=1+r_2^2-r_3^2$, $\xi=1-r_2^2+r_3^2$, $r_2=M_{D^{(*)+}}/M_B$, and $r_3=M_{K^{*0}}/M_B$ for vector meson K^{*0}. We set $r_3=0$ for the K^0 meson, since $m_K \ll m_B$. The longitudinal polarization vectors of the D^{*+} and K^{*0} are given as

$$\epsilon_{2L}=\frac{1}{2\sqrt{2}r_2}\left(\sqrt{\eta^2-4r_2^2}+\eta,\ \ \sqrt{\eta^2-4r_2^2}-\eta,\ \ \mathbf{0}_T\right),$$

$$\epsilon_{3L}=\frac{1}{2\sqrt{2}r_3}\left(\sqrt{\xi^2-4r_3^2}-\xi,\ \ \sqrt{\xi^2-4r_3^2}+\xi,\ \ \mathbf{0}_T\right), \tag{3}$$

respectively. The transverse polarization vectors can be adapted directly as $\epsilon_{2T}=(0,0,\mathbf{1}_T)$, $\epsilon_{3T}=(0,0,\mathbf{1}_T)$. We denote the light (anti)quark momenta in B^+, $D^{(*)+}$, and $K^{(*)0}$ mesons as $k_1=(x_1P_1^+,0,\mathbf{k}_{1T})$, $k_2=(x_2P_2^+,0,\mathbf{k}_{2T})$, and $k_3=(0,x_3P_3^-,\mathbf{k}_{3T})$, respectively. Integrating Eq. (1) over k_1^-, k_2^-, and k_3^+, we obtain

$$\text{amplitude}\sim\int dx_1dx_2dx_3b_1db_1b_2db_2b_3db_3 \tag{4}$$
$$\mathrm{Tr}[C(t)\Phi_B(x_1,b_1)\Phi_{D^{(*)}}(x_2,b_2)\Phi_{K^{(*)}}(x_3,b_3)$$
$$\times H(x_i,b_i,t)S_t(x_i)e^{-S(t)}],$$

where b_i is the conjugate space coordinate of k_{iT}, and t is the largest energy scale in H, as a function in terms of x_i and b_i. The large logarithms $\ln(M_W/t)$ resulting from QCD radiative corrections to four-quark operators are absorbed into the Wilson coefficients $C(t)$. The inclusion of k_T brings in one kind of large logarithms $\ln^2(Pb)$ from the overlap of collinear and soft gluon corrections, P denoting the dominant light-cone component of meson momentum. The other kind of large logarithms $\ln(tb)$ derives from the renormalization of the ultraviolet divergences. These two kinds of large logarithms are summed and lead to the Sudakov form factor $e^{-S(t)}$. It suppresses the soft dynamics effectively [13]. The large double logarithms $\ln^2 x_i$ are summed by the threshold resummation [14], and they lead to $S_t(x_i)$ which smears the end-point singularities on x_i. From the brief analysis above, it can be seen that PQCD is a consistent approach.

III. ANALYTIC FORMULAS

A. Wave functions

We use the wave functions $\Phi_{M,\alpha\beta}$ decomposed in terms of spin structure. The coming B meson and outgoing $D^{(*)+}$, $K^{(*)0}$ are as follows:

$$\Phi_B(x,b)=\frac{i}{\sqrt{2N_c}}[(\not P_1\gamma_5)+M_B\gamma_5]\phi_B(x,b), \tag{5}$$

$$\Phi_D(x,b)=\frac{i}{\sqrt{2N_c}}[\gamma_5(\not P_2+M_D)]\phi_D(x,b), \tag{6}$$

$$\Phi_{D^*}(x,b)=\frac{i}{\sqrt{2N_c}}[\not\epsilon(\not P_2+M_{D^*})]\phi_{D^*}(x,b), \tag{7}$$

$$\Phi_K(x,b)=\frac{i}{\sqrt{2N_c}}[\gamma_5\not P_3\phi_K^A(x,b)+M_{0K}\gamma_5\phi_K^P(x,b)$$
$$+M_{0K}\gamma_5(\not v\not n-1)\phi_K^T(x,b)], \tag{8}$$

$$\Phi_{K^*L}(x,b)=\frac{i}{\sqrt{2N_c}}[M_{K^*}\not\epsilon_{3L}\phi_{K^*}(x,b)+\not\epsilon_{3L}\not P_3\phi_{K^*}^t(x,b)$$
$$+M_{K^*}I\phi_{K^*}^s(x,b)], \tag{9}$$

$$\Phi_{K^*T}(x,b)=\frac{i}{\sqrt{2N_c}}\Bigg[M_{K^*}\not\epsilon_{3T}\Phi_{K^*}^v(x)+\not\epsilon_{3T}\not P_3\Phi_{K^*}^T(x)$$
$$+\frac{M_{K^*}}{P_3\cdot n}i\epsilon_{\mu\nu\rho\sigma}\gamma_5\gamma^\mu\epsilon_{3T}^\nu P_3^\rho n^\sigma\Phi_{K^*}^a(x)\Bigg], \tag{10}$$

where $N_c=3$ is color's degree of freedom, and $M_{0K}=M_{K'}^2/(m_u+m_s)$, $v=(0,1,\mathbf{0}_T)\propto P_3$, $n=(1,0,\mathbf{0}_T)$, and $\epsilon^{0123}=1$. The subscripts L and T denote the wave functions corresponding to the longitudinally and transversely polarized K^* mesons.

B. Effective Hamiltonian

The effective Hamiltonian for decay $B^+\to D^{(*)+}K^{(*)0}$ at a scale lower than M_W is given by [15]

$$H_{\rm eff}=\frac{G_F}{\sqrt{2}}V_{ub}^*V_{cs}[C_1(\mu)O_1(\mu)+C_2(\mu)O_2(\mu)], \tag{11}$$

$$O_1=(\overline{b}s)_{V-A}(\overline{c}u)_{V-A}, \quad O_2=(\overline{b}u)_{V-A}(\overline{c}s)_{V-A}, \tag{12}$$

where $C_{1,2}(\mu)$ are Wilson coefficients at renormalization scale μ, and summation in $SU(3)_c$ color's index α and chiral projection, $\Sigma_\alpha \overline{q}_\alpha \gamma^\nu(1-\gamma_5)q'_\alpha$, are abbreviated to $(\overline{q}q')_{V-A}$. The lowest order diagrams of $B^+\to D^{(*)}+K^{(*)0}$ are drawn in Fig. 1. We will choose $|V_{cs}|=0.996\pm0.013$, $|V_{ub}|=(3.6\pm0.7)\times10^{-3}$ [16]. There is no *CP* violation in the decays, since only one kind of Cabibbo-Kobayashi-Maskawa (CKM) phase appears in the processes. Therefore the decay width for the *CP*-conjugated mode, $B^-\to D^{(*)-}\overline{K}^{(*)0}$, equals $B^+\to D^{(*)+}K^{(*)0}$, respectively.

C. Decay width

The total decay amplitude for each mode or helicity state of $B^+\to D^{(*)+}K^{(*)0}$ is written as

$$A=f_B F+M, \tag{13}$$

where f_B is the decay constant of the B meson, and the overall factor is included in the decay width with the kinematics factor. $F(M)$ stands for the amplitude of (non)factorizable annihilation diagrams in Figs. 1a, 1b (1c, 1d). We exhibit their explicit expressions and subscripts of F and M according to the modes and helicity states, respectively, in the Appendix. It is noted that in the analytic formulas of amplitudes, we keep only the leading terms in the expansion of $r_2^2\sim0.15$ or $r_3^2\sim0.04$.[1] The decay width for each mode of these decays is given as

$$\Gamma=\frac{G_F^2M_B^3}{128\pi}(1-r_2^2)\sum_\sigma |V_{ub}^*V_{cs}A_\sigma|^2, \tag{14}$$

where the subscript σ denotes the helicity states of the two vector mesons with $L(T(1,2))$ standing for the longitudinal (transverse) component in the case of $B^+\to D^{*+}K^{*0}$ decay, as shown in the Appendix.

IV. NUMERICAL RESULTS

In the numerical analysis, we adopt the B meson wave function as [6,7]

$$\phi_B(x,b)=N_Bx^2(1-x)^2\exp\left[-\frac{M_B^2x^2}{2\omega_b^2}-\frac{1}{2}(\omega_b b)^2\right], \tag{15}$$

with the shape parameter ω_b and the normalization constant N_B being related to the decay constant f_B by normalization:

$$\int_0^1 dx\,\phi_M(x,b=0)=\frac{f_M}{2\sqrt{2N_c}}, \tag{16}$$

which is also right for the $D^{(*)}$ meson—i.e., $M=B,D^{(*)}$.

For the $D^{(*)}$ meson wave function, we use two types. The first kind [17] is

$$\text{(I)} \quad \phi_{D^{(*)}}(x)=\frac{3}{\sqrt{2N_c}}f_{D^{(*)}}x(1-x)\{1+a_{D^{(*)}}(1-2x)\}\times\exp\left[-\frac{1}{2}(\omega_{D^{(*)}}b)^2\right], \tag{17}$$

in which the last term $\exp[-\frac{1}{2}(\omega_{D^{(*)}}b)^2]$ is derived from the k_T distribution. By taking same parameters, we neglect the difference between the D and D^* mesons wave functions, since the c quark is much heavier than the $\overline{d}$ quark, and the mass difference between two mesons is little. The second kind [18] is

$$\text{(II)} \quad \phi_{D^{(*)}}(x)=\frac{3}{\sqrt{2N_c}}f_{D^{(*)}}x(1-x)\{1+a_{D^{(*)}}(1-2x)\}, \tag{18}$$

which is fitted from the measured $B\to D^{(*)}\ell\nu$ decay spectrum at large recoil. The absence of the last term like (I) is due to the insufficiency of the experiment data.

The $K^{(*)}$ wave functions [19,20] we adopt are calculated by QCD sum rules. To abridge the context, we list them and the corresponding parameters in the Appendix.

The other input parameters are listed below:

$$f_B=190\ \text{MeV},\quad f_D=240\ \text{MeV},\quad f_{D^*}=240\ \text{MeV},$$
$$f_K=160\ \text{MeV},\quad f_{K^*}=200\ \text{MeV},$$
$$f_{K^*}^T=160\ \text{MeV},\quad \omega_{D^{(*)}}=0.2\ \text{GeV}, \tag{19}$$
$$M_{0K}=1.60\ \text{GeV},\quad \omega_b=0.4\ \text{GeV},\quad a_{D^{(*)}}=0.3,$$
$$C_D=0.8,\quad C_{D^*}=0.7, \tag{20}$$
$$M_B=5.279\ \text{GeV},\quad M_b=4.8\ \text{GeV},$$
$$M_D=1.869\ \text{GeV},\quad M_{D^*}=2.010\ \text{GeV},$$
$$M_t=170\ \text{GeV},\quad M_W=80.4\ \text{GeV},$$
$$\tau_{B^\pm}=1.674\times10^{-12}\text{s},\quad G_F=1.16639\times10^{-5}\ \text{GeV}^{-2}, \tag{21}$$

where the Fermi coupling constant G_F, the masses, and lifetimes of particles refer to [21].

With the analytic formulas and parameters above, we get the branching ratios of $B^+\to D^{(*)+}K^{(*)0}$ shown in Tables I, II, III, and IV for two kinds of $D^{(*)}$ wave functions, respectively. The magnitude according to $D^{(*)}$ wave function *I* is about 60% of the one corresponding to the $D^{(*)}$ wave function II. The difference can tell the correct $D^{(*)}$ wave function by the experiment data in the future.

For each mode of $B^+\to D^{(*)+}K^{(*)0}$ decays, the contribution of the factorizable and nonfactorizable annihilation dia-

[1]This approximation is also adapted in deriving meson wave functions; see, for example, Ref. [20].

TABLE I. The branching ratios of the three decay modes and amplitudes (10^{-2} GeV) in terms of the factorizable, nonfactorizable diagrams and the sum of them according to the $D^{(*)}$ wave function I.

	$B\to DK$	$B\to D^*K$	$B\to DK^*$
f_BF	$-1.56+1.21i$	$-1.86+2.20i$	$1.17-1.65i$
M	$1.03+1.29i$	$-1.01-0.78i$	$-1.75-0.89i$
A	$-0.52+2.50i$	$-2.87+1.41i$	$-0.58-2.54i$
Br(10^{-6})	0.93	1.42	0.96

TABLE II. The branching ratios of $B\to D^*K^*$ decay and helicity amplitudes (10^{-2} GeV) in terms of the factorizable, nonfactorizable diagrams and the sum of them according to the D^* wave function I.

	$(B\to D^*K^*)_L$	$(B\to D^*K^*)_{T1}$	$(B\to D^*K^*)_{T2}$
f_BF	$-0.17-3.44i$	$1.58-3.47i$	$-0.37-0.22i$
M	$1.73+0.35i$	$-0.09-0.41i$	$0.009+0.005i$
A	$1.56-3.08i$	$1.49-3.87i$	$-0.36-0.21i$
Br(10^{-6})	1.67	2.40	0.02
Total Br(10^{-6})	4.09		

TABLE III. The branching ratios of the four decay modes and amplitudes (10^{-2} GeV) in terms of the factorizable, nonfactorizable diagrams and the sum of them according to the $D^{(*)}$ wave function II.

	$B\to DK$	$B\to D^*K$	$B\to DK^*$
f_BF	$-2.38+1.56i$	$-2.47+2.94i$	$1.50-2.32i$
M	$1.37+1.49i$	$-1.24-0.87i$	$-2.18-1.01i$
A	$-1.01+3.05i$	$-3.71+2.07i$	$-0.68-3.32i$
Br(10^{-6})	1.47	2.52	1.64

TABLE IV. The branching ratios of $B\to D^*K^*$ decay and helicity amplitudes (10^{-2} GeV) in terms of the factorizable, nonfactorizable diagrams and the sum of them according to the D^* wave function II.

	$(B\to D^*K^*)_L$	$(B\to D^*K^*)_{T1}$	$(B\to D^*K^*)_{T2}$
f_BF	$-0.38-4.61i$	$2.02-4.62i$	$-0.44-0.22i$
M	$2.03+0.37i$	$-0.14-0.49i$	$0.01+0.006i$
A	$1.65-4.24i$	$1.88-5.11i$	$-0.43-0.22i$
Br(10^{-6})	2.89	4.12	0.03
Total Br(10^{-6})	7.04		

TABLE V. The sensitivity of the branching ratio (10^{-6}) to the 30% extent of parameters in terms of the four modes of the $B^+\to D^{(*)+}K^{(*)0}$ decays according to the $D^{(*)}$ wave function I.

M_{0K}	Br($B\to DK$)	Br($B\to D^*K$)	Br($B\to DK^*$)	Br($B\to D^*K^*$)
1.12	0.79	0.81	–	–
1.60	0.93	1.42	–	–
2.08	1.09	2.22	–	–
ω_b	Br($B\to DK$)	Br($B\to D^*K$)	Br($B\to DK^*$)	Br($B\to D^*K^*$)
0.28	1.16	1.41	1.21	4.25
0.40	0.93	1.42	0.96	4.09
0.52	0.75	1.42	0.79	3.99
$a_{D^{(*)}}$	Br($B\to DK$)	Br($B\to D^*K$)	Br($B\to DK^*$)	Br($B\to D^*K^*$)
0.21	0.88	1.32	0.90	3.79
0.30	0.93	1.42	0.96	4.09
0.39	0.99	1.54	1.03	4.40

grams is the same order, although F is proportional to the Wilson coefficient $C_2+C_1/3$, which is $\mathcal{O}(1)$, and the nonfactorizable annihilation diagram contribution is proportional to C_1, which is about 30% of $C_2+C_1/3$. Since the counteraction influence between Figs. 1a, 1b of F is heavier than that between Figs. 1c, 1d of M by the reason of the more similar propagators in Figs. 1a, 1b. The magnitude comparison can be seen directly from Tables I, II, III, and IV.

From Tables II and IV, we can see $|A_{T1}|>|A_L|\gg|A_{T2}|$ in the case of the $B\to VV$ mode. There are two questions worthy of asking: Why is $|A_{T2}|$ so little? Why are $|A_{T1}|$ and $|A_L|$ the same order, though $|A_{T1}|$ is suppressed at least by the term r^2 ($r=r_2$ or r_3)? According to the amplitudes of F_{T2} and M_{T2}, the contribution of the twist-2 wave function ϕ_{K*}^T is absent, and the coefficients corresponding to the twist-3 wave functions ϕ_{K*}^v and ϕ_{K*}^a are just the opposite and counteract each other heavily. Therefore the value of A_{T2} is too little to consider. To answer the second question, we should note that r_2 is not a serious suppression term, especially when r_2 times 2, $2r_2\simeq 1$, like the term in F_{T1} and M_{T1}. In the case of F_{T1} and M_{T1}, all of the signs of the subamplitudes corresponding to the two twist-3 K^* wave functions are same, and the terms in the front of the twist-2 wave function ϕ_{K*}^T do not suffer the heavy suppression of r_3. On the other hand, in F_L (M_L) the seemly main contribution of the twist-2 wave function ϕ_{K*} is offset by the opposite coefficients in Figs. 1a, 1b (1c, 1d). Moreover in Fig. 1a the signs of the coefficients corresponding to the twist-3 wave function ϕ_{K*}^t and ϕ_{K*}^s are different. For the reasons above, $|A_{T1}|$ and $|A_L|$ are the same order.

It should be stressed that there is no arbitrary parameter in our calculation, but we only know the magnitude of each up to a range. In Tables V and VI we show the sensitivity of the branching ratios to 30% change of the parameters in Eq. (20) according to the two kinds of $D^{(*)}$ wave functions, respectively. Since the M_{0K} and ω_b uncertainty influences the results very much, we will limit them to a more appropriate extent. According to [19],

TABLE VI. The sensitivity of the branching ratio (10^{-6}) to the 30% extent of parameters in terms of the four modes of the $B^+\to D^{(*)+}K^{(*)0}$ decays according to the $D^{(*)}$ wave function II.

M_{0K}	$\mathrm{Br}(B\to DK)$	$\mathrm{Br}(B\to D^*K)$	$\mathrm{Br}(B\to DK^*)$	$\mathrm{Br}(B\to D^*K^*)$
1.12	1.17	1.41	–	–
1.60	1.47	2.52	–	–
2.08	1.80	3.95	–	–
ω_b	$\mathrm{Br}(B\to DK)$	$\mathrm{Br}(B\to D^*K)$	$\mathrm{Br}(B\to DK^*)$	$\mathrm{Br}(B\to D^*K^*)$
0.28	1.86	2.48	2.06	7.22
0.40	1.47	2.52	1.64	7.04
0.52	1.20	2.51	1.34	6.92
C_D	$\mathrm{Br}(B\to DK)$	$\mathrm{Br}(B\to D^*K)$	$\mathrm{Br}(B\to DK^*)$	$\mathrm{Br}(B\to D^*K^*)$
0.56	1.26	–	1.38	–
0.80	1.47	–	1.64	–
1.04	1.70	–	1.92	–
C_{D*}	$\mathrm{Br}(B\to DK)$	$\mathrm{Br}(B\to D^*K)$	$\mathrm{Br}(B\to DK^*)$	$\mathrm{Br}(B\to D^*K^*)$
0.49	–	2.13	–	5.99
0.70	–	2.52	–	7.04
0.91	–	2.95	–	7.50

$$1.4\ \mathrm{GeV}\leqslant M_{0K}\leqslant 1.8\ \mathrm{GeV}, \tag{22}$$

the branching ratios are

$$\mathrm{Br}(B^+\to D^+K^0)=\begin{cases}0.93^{+0.06}_{-0.06}\times 10^{-6} & (\mathrm{I}),\\ 1.47^{+0.13}_{-0.13}\times 10^{-6} & (\mathrm{II}),\end{cases} \tag{23}$$

$$\mathrm{Br}(B^+\to D^{*+}K^0)=\begin{cases}1.42^{+0.31}_{-0.27}\times 10^{-6} & (\mathrm{I}),\\ 2.52^{+0.55}_{-0.50}\times 10^{-6} & (\mathrm{II}),\end{cases} \tag{24}$$

where I(II) stands for the result for I(II) kind of $D^{(*)}$ wave function. From the $B\to K$ transition form factor $f_+^K(0)$, we can limit the appropriate extent of ω_b. $f_+^K(0)$ calculated from PQCD at $m_{0K}=1.6$ GeV is consistent with $f_+^K(0)$ by QCD sum rules [19], when

$$0.35\ \mathrm{GeV}\leqslant \omega_b\leqslant 0.46\ \mathrm{GeV}. \tag{25}$$

In the above range, the branching ratios are

$$\mathrm{Br}(B^+\to D^+K^0)=\begin{cases}0.93^{+0.09}_{-0.10}\times 10^{-6} & (\mathrm{I}),\\ 1.47^{+0.15}_{-0.15}\times 10^{-6} & (\mathrm{II}),\end{cases} \tag{26}$$

$$\mathrm{Br}(B^+\to D^{*+}K^0)=\begin{cases}1.42^{+0.00}_{-0.00}\times 10^{-6} & (\mathrm{I}),\\ 2.52^{+0.00}_{-0.01}\times 10^{-6} & (\mathrm{II}),\end{cases} \tag{27}$$

$$\mathrm{Br}(B^+\to D^+K^{*0})=\begin{cases}0.96^{+0.10}_{-0.09}\times 10^{-6} & (\mathrm{I}),\\ 1.64^{+0.16}_{-0.17}\times 10^{-6} & (\mathrm{II}),\end{cases} \tag{28}$$

$$\mathrm{Br}(B^+\to D^{*+}K^{*0})=\begin{cases}4.09^{+0.06}_{-0.06}\times 10^{-6} & (\mathrm{I}),\\ 7.04^{+0.07}_{-0.06}\times 10^{-6} & (\mathrm{II}).\end{cases} \tag{29}$$

Besides the perturbative annihilation contribution above, there is also contribution from the final state interaction (FSI) in the hadronic level, such as $B^+\to D^{(*)0}K^{(*)+}$ then $D^{(*)0}K^{(*)+}\to D^{(*)+}K^{(*)0}$. Based on the argument of color transparency [9,22], FSI effects may not be important in the two-body B decays. So we suppose that the dominant contribution is what we calculated above. The hypothesis is consistent with the argument in [6,23].

V. CONCLUSION

In this paper, we study the four modes of $B^+\to D^{(*)+}K^{(*)0}$ decays. Based on the consistent PQCD framework, we predict the branching ratios of these pure annihilation-type decays of the order of 10^{-6} and show the theoretical errors. Such results can be measured in the two B factories in the future.

ACKNOWLEDGMENTS

We thank Y. Li for beneficial discussions. This work is partly supported by the National Science Foundation of China under contracts 90103013 and 10135060.

APPENDIX A: THE (NON)FACTORIZABLE AMPLITUDE

At first order of α_s, we get the analytic formulas of the (non)factorizable amplitude for each mode or helicity state listed below. We neglect the small term x_1 in the numerators of the hard part of M, since the B meson wave function in Eq. (15) has a sharp peak at the small x region, $\mathcal{O}(\bar{\Lambda}/M_B)$, where $\bar{\Lambda}\equiv M_B-M_b$. It should be noticed that we do not employ this approximation to the denominators of the propagator which are sensitive to x_1 because x_1 there behaves as a cutoff. We also neglect terms higher than $r_{1,2}^2$ orders, since the light cone wave functions derived from sum rules are expanded to this order [20].

1. $B^+\to D^+K^0$ decay

The amplitude for the factorizable annihilation diagrams in Figs. 1a, 1b is given as

$$F_1=16\pi C_F M_B^2\int_0^1 dx_2 dx_3\int_0^\infty b_2 db_2 b_3 db_3 \phi_D(x_2,b_2)[\{(x_3-2x_3r_2^2-r_2^2)\phi_K^A(x_3,b_3)+r_2r_K(1+2x_3)\phi_K^P(x_3,b_3)-r_2r_K(1-2x_3)\phi_K^T(x_3,b_3)\}E_f(t_a^1)h_a(x_2,x_3,b_2,b_3)+\{(r_2^2-1)x_2\phi_K^A(x_3,b_3)-2r_2r_K(1+x_2)\phi_K^P(x_3,b_3)\}E_f(t_a^2)h_a(x_3,x_2,b_3,b_2)]. \tag{A1}$$

The amplitude for the nonfactorizable annihilation diagrams in Figs. 1c, 1d is obtained as

$$M_1=-\frac{1}{\sqrt{2N_c}}64\pi C_F M_B^2\int_0^1 dx_1dx_2dx_3\int_0^\infty b_1db_1b_2db_2\phi_B(x_1,b_1)\phi_D(x_2,b_2)(\{[x_3+(x_2-2x_3-1)r_2^2]\phi_K^A(x_3,b_2)+r_2r_K(2+x_2+x_3)\phi_K^P(x_3,b_2)-r_2r_K(x_2-x_3)\phi_K^T(x_3,b_2)\}E_m(t_m^1)h_a^{(1)}(x_1,x_2,x_3,b_1,b_2)-\{x_2\phi_K^A(x_3,b_2)+r_2r_K(x_2+x_3)\phi_K^P(x_3,b_2)+r_2r_K(x_2-x_3)\phi_K^T(x_3,b_2)\}E_m(t_m^2)h_a^{(2)}(x_1,x_2,x_3,b_1,b_2)), \tag{A2}$$

where $C_F=4/3$ is the group factor of $SU(3)_c$ gauge group, $r_K=M_{0K}/M_B$, and the functions E_f, E_m, $t_a^{1,2}$, h_a are given in Appendix C.

2. $B^+\to D^{*+}K^0$ decay

$$F_2=-16\pi C_F M_B^2\int_0^1 dx_2dx_3\int_0^\infty b_2db_2b_3db_3\phi_{D*}(x_2,b_2)[\{(x_3-2x_3r_2^2+r_2^2)\phi_K^A(x_3,b_3)+r_2r_K\phi_K^P(x_3,b_3)-r_2r_K\phi_K^T(x_3,b_3)\}E_f(t_a^1)h_a(x_2,x_3,b_2,b_3)-\{(1-r_2^2)x_2\phi_K^A(x_3,b_3)-2r_2r_K(1-x_2)\phi_K^P(x_3,b_3)\}E_f(t_a^2)h_a(x_3,x_2,b_3,b_2)], \tag{A3}$$

$$M_2=\frac{1}{\sqrt{2N_c}}64\pi C_F M_B^2\int_0^1 dx_1dx_2dx_3\int_0^\infty b_1db_1b_2db_2\phi_B(x_1,b_1)\phi_{D*}(x_2,b_2)(\{[x_3+(1-x_2-2x_3)r_2^2]\phi_K^A(x_3,b_2)+r_2r_K(x_3-x_2)\phi_K^P(x_3,b_2)-r_2r_K(2-x_2-x_3)\phi_K^T(x_3,b_2)\}E_m(t_m^1)h_a^{(1)}(x_1,x_2,x_3,b_1,b_2)-\{(1-2r_2^2)x_2\phi_K^A(x_3,b_2)+r_2r_K(x_2-x_3)\phi_K^P(x_3,b_2)+r_2r_K(x_2+x_3)\phi_K^T(x_3,b_2)\}E_m(t_m^2)h_a^{(2)}(x_1,x_2,x_3,b_1,b_2)). \tag{A4}$$

3. $B^+\to D^+K^{*0}$ decay

$$F_3=-16\pi C_F M_B^2\int_0^1 dx_2dx_3\int_0^\infty b_2db_2b_3db_3\phi_D(x_2,b_2)[\{(x_3-2x_3r_2^2-r_2^2)\phi_{K*}(x_3,b_3)+r_2r_3(1+2x_3)\phi_{K*}^s(x_3,b_3)-r_2r_3(1-2x_3)\phi_{K*}^t(x_3,b_3)\}E_f(t_a^1)h_a(x_2,x_3,b_2,b_3)-\{(1-r_2^2)x_2\phi_{K*}(x_3,b_3)+2r_2r_3(1+x_2)\phi_{K*}^s(x_3,b_3)\}E_f(t_a^2)h_a(x_3,x_2,b_3,b_2)], \tag{A5}$$

$$M_3=\frac{1}{\sqrt{2N_c}}64\pi C_F M_B^2\int_0^1 dx_1dx_2dx_3\int_0^\infty b_1db_1b_2db_2\phi_B(x_1,b_1)\phi_D(x_2,b_2)(\{[x_3+(x_2-2x_3-1)r_2^2]\phi_{K*}(x_3,b_2)+r_2r_3(2+x_2+x_3)\phi_{K*}^s(x_3,b_2)-r_2r_3(x_2-x_3)\phi_{K*}^t(x_3,b_2)\}E_m(t_m^1)h_a^{(1)}(x_1,x_2,x_3,b_1,b_2)-\{x_2\phi_{K*}(x_3,b_2)+r_2r_3(x_2+x_3)\phi_{K*}^s(x_3,b_2)+r_2r_3(x_2-x_3)\phi_{K*}^t(x_3,b_2)\}E_m(t_m^2)h_a^{(2)}(x_1,x_2,x_3,b_1,b_2)). \tag{A6}$$

4. $B^+\to D^{*+}K^{*0}$ decay

$$F_L=16\pi C_F M_B^2\int_0^1 dx_2dx_3\int_0^\infty b_2db_2b_3db_3\phi_{D*}(x_2,b_2)[\{(x_3-2x_3r_2^2+r_2^2)\phi_{K*}(x_3,b_3)+r_2r_3\phi_{K*}^s(x_3,b_3)-r_2r_3\phi_{K*}^t(x_3,b_3)\}E_f(t_a^1)h_a(x_2,x_3,b_2,b_3)-\{(1-r_2^2)x_2\phi_{K*}(x_3,b_3)+2r_2r_3(x_2-1)\phi_{K*}^s(x_3,b_3)\}E_f(t_a^2)h_a(x_3,x_2,b_3,b_2)], \tag{A7}$$

$$M_L = \frac{1}{\sqrt{2N_c}} 64\pi C_F M_B^2 \int_0^1 dx_1 dx_2 dx_3 \int_0^\infty b_1 db_1 b_2 db_2 \phi_B(x_1,b_1)\phi_{D*}(x_2,b_2)(\{[-x_3+(x_2+2x_3-1)r_2^2]\phi_{K*}(x_3,b_2)$$
$$+r_2r_3(x_2-x_3)\phi^s_{K*}(x_3,b_2)+r_2r_3(2-x_2-x_3)\phi^t_{K*}(x_3,b_2)\}E_m(t_m^1)h_a^{(1)}(x_1,x_2,x_3,b_1,b_2)+\{(1-2r_2^2)x_2\phi_{K*}(x_3,b_2)$$
$$+r_2r_3(x_2-x_3)\phi^s_{K*}(x_3,b_2)+r_2r_3(x_2+x_3)\phi^t_{K*}(x_3,b_2)\}E_m(t_m^2)h_a^{(2)}(x_1,x_2,x_3,b_1,b_2)), \tag{A8}$$

$$F_{T1} = 16\pi C_F M_B^2 \int_0^1 dx_2 dx_3 \int_0^\infty b_2 db_2 b_3 db_3 \phi_{D*}(x_2,b_2)[\{-2r_2r_3x_3\phi^v_{K*}(x_3,b_3)-2r_2r_3x_3\phi^a_{K*}(x_3,b_3)$$
$$+2r_2^2\phi^T_{K*}(x_3,b_3)\}E_f(t_a^1)h_a(x_2,x_3,b_2,b_3)+\{2r_2r_3\phi^v_{K*}(x_3,b_3)+2r_2r_3\phi^a_{K*}(x_3,b_3)\}E_f(t_a^2)h_a(x_3,x_2,b_3,b_2)], \tag{A9}$$

$$M_{T1} = \frac{1}{\sqrt{2N_c}} 64\pi C_F M_B^2 \int_0^1 dx_1 dx_2 dx_3 \int_0^\infty b_1 db_1 b_2 db_2 \phi_B(x_1,b_1)\phi_{D*}(x_2,b_2)[\{2r_2r_3\phi^v_{K*}(x_3,b_2)+2r_2r_3\phi^a_{K*}(x_3,b_2)$$
$$-2r_2^2(1-x_2)\phi^T_{K*}(x_3,b_2)\}E_m(t_m^1)h_a^{(1)}(x_1,x_2,x_3,b_1,b_2)-\{2r_2^2x_2\phi^T_{K*}(x_3,b_2)\}E_m(t_m^2)h_a^{(2)}(x_1,x_2,x_3,b_1,b_2)], \tag{A10}$$

$$F_{T2} = 16\pi C_F M_B^2 \int_0^1 dx_2 dx_3 \int_0^\infty b_2 db_2 b_3 db_3 \phi_{D*}(x_2,b_2)[\{-2r_2r_3\phi^v_{K*}(x_3,b_3)+2r_2r_3\phi^a_{K*}(x_3,b_3)\}E_f(t_a^1)h_a(x_2,x_3,b_2,b_3)$$
$$+\{2r_2r_3x_2\phi^v_{K*}(x_3,b_3)-2r_2r_3x_2\phi^a_{K*}(x_3,b_3)\}E_f(t_a^2)h_a(x_3,x_2,b_3,b_2)], \tag{A11}$$

$$M_{T2} = \frac{1}{\sqrt{2N_c}} 64\pi C_F M_B^2 \int_0^1 dx_1 dx_2 dx_3 \int_0^\infty b_1 db_1 b_2 db_2 \phi_B(x_1,b_1)\phi_{D*}(x_2,b_2)\{2r_2r_3\phi^v_{K*}(x_3,b_2)$$
$$-2r_2r_3\phi^a_{K*}(x_3,b_2)\}E_m(t_m^1)h_a^{(1)}(x_1,x_2,x_3,b_1,b_2), \tag{A12}$$

where the subscript $L(T(1,2))$—i.e., the helicity states of the two vector mesons σ in Eq. (14)—stands for the longitudinal (transverse) component, respectively. Conveniently we choose the polarization state $T1$ as $\epsilon_{2T}=(1/\sqrt{2})(0,0,1,i)$, $\epsilon_{3T}=(1/\sqrt{2})(0,0,1,-i)$, $T2$ as $\epsilon_{2T}=(1/\sqrt{2})(0,0,1,-i)$, and $\epsilon_{3T}=(1/\sqrt{2})(0,0,1,i)$. Each amplitude A_σ also is the sum of two parts, factorizable and nonfactorizable diagrams, related by Eq. (13).

APPENDIX B: THE $K^{(*)}$ MESON WAVE FUNCTIONS

The K and K^* meson wave functions are given as

$$\phi_K^A(x) = \frac{f_K}{2\sqrt{2N_c}} 6x(1-x)\{1+0.51(1-2x)$$
$$+0.2C_2^{3/2}(1-2x)\}, \tag{B1}$$

$$\phi_K^P(x) = \frac{f_K}{2\sqrt{2N_c}}\{1+0.212C_2^{1/2}(1-2x)$$
$$-0.148C_4^{1/2}(1-2x)\}, \tag{B2}$$

$$\phi_K^T(x) = \frac{f_K}{2\sqrt{2N_c}}(1-2x)\{1+0.1581[-3+5(1-2x)^2]\}, \tag{B3}$$

$$\Phi_{K*}(x) = \frac{f_{K*}}{2\sqrt{2N_c}} 6x(1-x)[1+0.57(1-2x)$$
$$+0.07C_2^{3/2}(1-2x)], \tag{B4}$$

$$\Phi^t_{K*}(x) = \frac{f^T_{K*}}{2\sqrt{2N_c}}(0.3(1-2x)[3(1-2x)^2$$
$$+10(1-2x)-1]+1.68C_4^{1/2}(1-2x)$$
$$+0.06(1-2x)^2[5(1-2x)^2-3]$$
$$+0.36\{1-2(1-2x)[1+\ln(1-x)]\}), \tag{B5}$$

$$\Phi^s_{K^*}(x)=\frac{f^T_{K^*}}{2\sqrt{2N_c}}\{3(1-2x)[1+0.2(1-2x)+0.6(10x^2-10x+1)]-0.12x(1-x)+0.36[1-6x-2\ln(1-x)]\}, \tag{B6}$$

$$\Phi^T_{K^*}(x)=\frac{f^T_{K^*}}{2\sqrt{2N_c}}6x(1-x)[1+0.6(1-2x)+0.04C_2^{3/2}(1-2x)], \tag{B7}$$

$$\Phi^v_{K^*}(x)=\frac{f_{K^*}}{2\sqrt{2N_c}}\left\{\frac{3}{4}[1+(1-2x)^2+0.44(1-2x)^3]+0.4C_2^{1/2}(1-2x)+0.88C_4^{1/2}(1-2x)+0.48[2x+\ln(1-x)]\right\}, \tag{B8}$$

$$\Phi^a_{K^*}(x)=\frac{f_{K^*}}{4\sqrt{2N_c}}\{3(1-2x)[1+0.19(1-2x)+0.81(10x^2-10x+1)]-1.14x(1-x)+0.48[1-6x-2\ln(1-x)]\}, \tag{B9}$$

with the Gegenbauer polynomials,

$$C_2^{1/2}(\xi)=\frac{1}{2}(3\xi^2-1),\quad C_4^{1/2}(\xi)=\frac{1}{2}(35\xi^4-30\xi^2+3),$$
$$C_2^{3/2}(\xi)=\frac{3}{2}(5\xi^2-1). \tag{B10}$$

APPENDIX C: SOME USED FORMULAS

The definitions of some functions used in the text are presented in this appendix. In the numerical analysis we use the one-loop expression for the strong coupling constant,

$$\alpha_s(\mu)=\frac{4\pi}{\beta_0\ln(\mu^2/\Lambda^2)}, \tag{C1}$$

where $\beta_0=(33-2n_f)/3$ and n_f is number of active flavor at appropriate scale. Λ is the QCD scale, which we use as 250 MeV at $n_f=4$. We also use leading logarithm expressions for the Wilson coefficients $C_{1,2}$ presented in Ref. [15].

The functions E_f and E_m including Wilson coefficients are defined as

$$E_f(t)=a(t)\alpha_s(t)e^{-S_D(t)-S_K(t)}, \tag{C2}$$

$$E_m(t)=C_1(t)\alpha_s(t)e^{-S_B(t)-S_D(t)-S_K(t)}\big|_{b_3=b_2}, \tag{C3}$$

where

$$a(t)=C_2(t)+\frac{C_1(t)}{N_c}, \tag{C4}$$

and S_B, S_D, and S_K result from summing both double logarithms caused by soft gluon corrections and single ones due to the renormalization of ultraviolet divergence. The above $S_{B,D,K}$ are defined as

$$S_B(t)=s(x_1P_1^+,b_1)+2\int_{1/b_1}^t\frac{d\mu'}{\mu'}\gamma_q(\mu'), \tag{C5}$$

$$S_D(t)=s(x_2P_2^+,b_3)+2\int_{1/b_2}^t\frac{d\mu'}{\mu'}\gamma_q(\mu'), \tag{C6}$$

$$S_K(t)=s(x_3P_3^-,b_3)+s((1-x_3)P_3^-,b_3)+2\int_{1/b_3}^t\frac{d\mu'}{\mu'}\gamma_q(\mu'), \tag{C7}$$

where $s(Q,b)$, so-called Sudakov factor, is given as [24]

$$s(Q,b)=\int_{1/b}^Q\frac{d\mu'}{\mu'}\left[\left\{\frac{2}{3}(2\gamma_E-1-\ln 2)+C_F\ln\frac{Q}{\mu'}\right\}\frac{\alpha_s(\mu')}{\pi}+\left\{\frac{67}{9}-\frac{\pi^2}{3}-\frac{10}{27}n_f+\frac{2}{3}\beta_0\ln\frac{e^{\gamma_E}}{2}\right\}\times\left(\frac{\alpha_s(\mu')}{\pi}\right)^2\ln\frac{Q}{\mu'}\right], \tag{C8}$$

where $\gamma_E=0.57722\ldots$ is Euler constant, and $\gamma_q=-\alpha_s/\pi$ is the quark anomalous dimension.

The functions h_a, $h_a^{(1)}$, and $h_a^{(2)}$ in the decay amplitudes consist of two parts: one is the jet function $S_t(x_i)$ derived by the threshold resummation [14], and the other is the propagator of virtual quark and gluon. They are defined by

$$h_a(x_2,x_3,b_2,b_3)=S_t(1-x_3)\left(\frac{\pi i}{2}\right)^2H_0^{(1)}[M_B\sqrt{(1-r_2^2)x_2x_3}b_2] \tag{C9}$$

$$\times\{H_0^{(1)}[M_B\sqrt{(1-r_2^2)x_3}b_2]J_0[M_B\sqrt{(1-r_2^2)x_3}b_3]\times\theta(b_2-b_3)+(b_2\leftrightarrow b_3)\}, \tag{C10}$$

$$h_a^{(j)}(x_1,x_2,x_3,b_1,b_2) = \left\{ \frac{\pi i}{2} H_0^{(1)}(M_B\sqrt{(1-r_2^2)x_2x_3}b_1) \times J_0(M_B\sqrt{(1-r_2^2)x_2x_3}b_2)\,\theta(b_1-b_2) + (b_1 \leftrightarrow b_2) \right\} \times \begin{pmatrix} K_0(M_B F_{(j)} b_1), & \text{for } F_{(j)}^2>0 \\ \frac{\pi i}{2} H_0^{(1)}(M_B\sqrt{|F_{(j)}^2|}b_1), & \text{for } F_{(j)}^2<0 \end{pmatrix}, \quad \text{(C11)}$$

where $H_0^{(1)}(z) = J_0(z) + iY_0(z)$, and $F_{(j)}$'s are defined by

$$F_{(1)}^2 = x_1 + x_2 + (1-x_1-x_2)x_3(1-r_2^2), \quad \text{(C12)}$$

$$F_{(2)}^2 = x_3(x_1-x_2)(1-r_2^2). \quad \text{(C13)}$$

We adopt the parametrization for $S_t(x)$ of the factorizable contributions:

$$S_t(x) = \frac{2^{1+2c}\Gamma(3/2+c)}{\sqrt{\pi}\Gamma(1+c)}[x(1-x)]^c, \quad c=0.3. \quad \text{(C14)}$$

In the nonfactorizable annihilation contributions, $S_t(x)$ gives a very small numerical effect to the amplitude [14]. Therefore, we drop $S_t(x)$ in $h_a^{(1)}$ and $h_a^{(2)}$. The hard scale t's in the amplitudes are taken as the largest energy scale in the H to destroy the large logarithmic radiative corrections:

$$t_a^1 = \max(M_B\sqrt{(1-r_2^2)x_3}, 1/b_2, 1/b_3), \quad \text{(C15)}$$

$$t_a^2 = \max(M_B\sqrt{(1-r_2^2)x_2}, 1/b_2, 1/b_3), \quad \text{(C16)}$$

$$t_m^j = \max(M_B\sqrt{|F_{(j)}^2|}, M_B\sqrt{(1-r_2^2)x_2x_3}, 1/b_1, 1/b_2). \quad \text{(C17)}$$

[1] M. Wirbel, B. Stech, and M. Bauer, Z. Phys. C **29**, 637 (1985); M. Bauer, B. Stech, and M. Wirbel, *ibid.* **34**, 103 (1987); L.-L. Chau, H.-Y. Cheng, W.K. Sze, H. Yao, and B. Tseng, Phys. Rev. D **43**, 2176 (1991); **58**, 019902(E) (1998).

[2] A. Ali, G. Kramer, and C.D. Lü, Phys. Rev. D **58**, 094009 (1998); C.D. Lü, Nucl. Phys. B (Proc. Suppl.) **74**, 227 (1999); Y.-H. Chen, H.-Y. Cheng, B. Tseng, and K.-C. Yang, Phys. Rev. D **60**, 094014 (1999); H.-Y. Cheng and K.-C. Yang, *ibid.* **62**, 054029 (2000).

[3] H.Y. Cheng, H.-n. Li, and K.C. Yang, Phys. Rev. D **60**, 094005 (1999).

[4] T.W. Yeh and H.-n. Li, Phys. Rev. D **56**, 1615 (1997).

[5] M. Beneke, G. Buchalla, M. Neubert, and C.T. Sachrajda, Phys. Rev. Lett. **83**, 1914 (1999); Nucl. Phys. **B591**, 313 (2000).

[6] Y.-Y. Keum, H.-n. Li, and A.I. Sanda, Phys. Lett. B **504**, 6 (2001); Phys. Rev. D **63**, 054008 (2001).

[7] C.-D. Lü, K. Ukai, and M.-Z. Yang, Phys. Rev. D **63**, 074009 (2001); C.-D. Lü, in *Proceedings of International Conference on Flavor Physics* (ICFP 2001), edited by W. L. Wu (World Scientific, Singapore, 2001), pp. 173–184.

[8] G.P. Lepage and S.J. Brodsky, Phys. Lett. **87B**, 359 (1979).

[9] G.P. Lepage and S.J. Brodsky, Phys. Rev. D **22**, 2157 (1980).

[10] C.-H.V. Chang and H.-n. Li, Phys. Rev. D **55**, 5577 (1997); T.-W. Yeh and H.-n. Li, *ibid.* **56**, 1615 (1997).

[11] H.-n. Li, Phys. Rev. D **64**, 014019 (2001); S. Mishima, Phys. Lett. B **521**, 252 (2001); E. Kou and A.I. Sanda, *ibid.* **525**, 240 (2002); C.-H. Chen, Y.-Y. Keum, and H.-n. Li, Phys. Rev. D **64**, 112002 (2001); C.-D. Lü and M.Z. Yang, Eur. Phys. J. C **23**, 275 (2002); A.I. Sanda and K. Ukai, Prog. Theor. Phys. **107**, 421 (2002); C.-H. Chen, Y.-Y. Keum, and H.-n. Li, Phys. Rev. D **66**, 054013 (2002); M. Nagashima and H.-n. Li, hep-ph/0202127; Y.-Y. Keum, hep-ph/0209002; hep-ph/0209208; hep-ph/0210127; Y.-Y. Keum and A.I. Sanda, Phys. Rev. D **67**, 054009 (2003).

[12] C.D. Lü, Eur. Phys. J. C **24**, 121 (2002); Y. Li and C.D. Lü, J. Phys. G **29**, 2115 (2003); High Energy Phys. Nucl. Phys. **27**, 1062 (2003); hep-ph/0308243; C.D. Lü and K. Ukai, Eur. Phys. J. C **28**, 305 (2003).

[13] H.-n. Li and B. Tseng, Phys. Rev. D **57**, 443 (1998).

[14] H.-n. Li, Phys. Rev. D **66**, 094010 (2002); H.-n. Li and K. Ukai, Phys. Lett. B **555**, 197 (2003).

[15] G. Buchalla, A.J. Buras, and M.E. Lautenbacher, Rev. Mod. Phys. **68**, 1125 (1996).

[16] Review of Particle Physics, K. Hagiwara *et al.*, Phys. Rev. D **66**, 010001 (2002).

[17] T. Kurimoto, H.-n. Li, and A.I. Sanda, Phys. Rev. D **67**, 054028 (2003).

[18] Y.-Y. Keum, T. Kurimoto, H.-N. Li, C.-D. Lü, and A.I. Sanda, Phys. Rev. D **69**, 094018 (2004).

[19] P. Ball, J. High Energy Phys. **09**, 005 (1998); **01**, 010 (1999).

[20] P. Ball, V.M. Braun, Y. Koike, and K. Tanaka, Nucl. Phys. **B529**, 323 (1998); P. Ball and V.M. Braun, hep-ph/9808229.

[21] Particle Data Group, Phys. Rev. D **66**, 010001 (2002).

[22] J.D. Bjorken, Nucl. Phys. B (Proc. Suppl.) **11**, 325 (1989).

[23] C.-H. Chen and H.-n. Li, Phys. Rev. D **63**, 014003 (2001).

[24] H.-n. Li and B. Melic, Eur. Phys. J. C **11**, 695 (1999).